*Research paper*

# Experimental Study of the Violence Intensity Parameters of the Explosion of Micron-sized Zinc Powder

## Yu Shu[*], Zijun Li[**]

*School of Resources and Safety Engineering,*
*Central South University, No. 932* South *Lushan Road,*
*Changsha Hunan 410083, P.R. China*
*E-mails*: [*]shuyu1994@csu.edu.cn; [**]zijunli@csu.edu.cn

**Abstract:** The focus of this study was the explosion hazard of micron-sized zinc powder in a small space and low energy environment in the actual using of ventilation pipes of zinc powder processing plants. In the experimental study, the dust explosion parameters in the device (20 L sphere) under special conditions was used, and zinc powder with a median diameter of 3.80 μm was the research material. The experimental conditions were at a temperature 296.15~299.15 K, and a humidity 45~55%. The dust explosion violence parameter of the micron-sized zinc powder was measured. The experimental results showed that when the energy of the igniter was 10 J and the explosion violence parameters of micron-sized zinc powder dust were largest, the ignition delay time was 162~165 ms, the pressure for powder injection was 1.19~1.21 MPa, and the dust concentration was 1750~1820 g/m$^3$. The experimental data were processed by the fitting method, and the degree of influence of three factors on the explosion intensity parameter of micron-sized zinc powder was as follows: dust concentration, ignition delay time, pressure for powder injection. These results are valuable in the design of explosion hazard assessment and anti-explosion measures in zinc powder production.

**Keywords:** dust explosion, micron-sized powder, zinc, maximum explosion pressure, maximum rate of pressure increase

### Nomenclature:

$d$     dust concentration, [g/m³]

$e$     universal constant, $e = 2.71828$

$P_0$    initial pressure [Pa]

$R$     radius of the container [m]

$S_C$    burning rate [m/s]

$x$     ignition delay time [ms]

$x_I$    pressure for powder injection [MPa]

$y$     maximum explosion pressure [MPa]

$y_R$    maximum rate of pressure increase [MPa/s]

$\gamma$     ratio of the specific heat capacities

## 1   Introduction

In the field of industrial explosion protection, dust is a general term for fine particles of solid matter [1-4]. A dust explosion is an explosion phenomenon when a certain concentration of combustible dust is dispersed in a combustion supporting environment and ignited by a suitable ignition energy in a limited space [5-7]. Since dust explosions occur in a relatively limited space, dust explosions generate large pressures and high temperatures in a short period of time and release a large amount of energy, so the risk of a dust explosion is very high.

The understanding of dust explosions can be traced back to 1785 [8]. The world's first recorded dust explosion occurred at a flour mill in Turien, Italy [9]. With the development of industrial modernization, the number of dust explosion accidents has increased, and people began to realize the danger of dust explosions. Thousands of dust explosions occur in China and abroad every year. A large number of these explosions will cause huge casualties, property loss and environmental hazards [10-12]. The high incidence and serious harm of dust explosion accidents have led to research on the parameters of the violence intensity of industrial dust explosions, and has become a research hotspot [13-18]. Li et al. [19] used a 20 L sphere explosion test device to study the explosion severity and flame propagation characteristics of micro-scale aluminum powder. Zhang et al. [20] studied the effect of turbulence on the explosion of different concentrations of aluminum powder in air. When the nominal concentration is low, turbulence is the main factor affecting the explosion, and when the nominal concentration is high, the uniformity of the aluminum powder distribution is the main factor affecting the explosion. Choi et al. [21] used Hartmann tubes

to study the effect of inert nitrogen on the minimum ignition energy of magnesium powder. Marmo *et al.* [22] explained the explosion hazard of aluminum powder in dust collection and removal devices in conjunction with actual cases.

Metal powder occupies a large proportion of many flammable dusts, and the high temperature and high pressure generated instantaneously during the explosion will cause great damage to surrounding buildings and personnel. Zinc powder is mostly a deflagration accident, and its explosion accident is rare. Therefore, there are few studies on the explosion characteristics of zinc powder. However, the multiple occurrence of deflagration accidents indicates that they are potentially explosive. Therefore, the destructiveness of zinc powder explosions has high research value. The results of this research can provide theoretical guidance for relevant industrial safety production, and thus provide effective recommendations for reducing the incidence of dust explosion accidents.

The dust explosion violence parameter is an important basis for the evaluation of explosion hazards and explosion protection, including the maximum explosion pressure and the maximum rate of pressure increase [10, 23, 24]. It mainly displays the hazards caused by dust explosions and is mostly used for the danger classification of dust.

Zinc powder is a micron-sized metal dust that has a wide range of uses in the chemical industry, coatings industry, and medical and health industries. Therefore, the present study uses zinc powder as an experimental material to systematically study and analyze its maximum explosion pressure and maximum rate of pressure increase. It is hoped that it can serve as reference in the formulation of explosion protection measures in the same kind of zinc powder production.

## 2 Experimental

### 2.1 Experimental materials

The zinc powder samples in these experiment were purchased from Shanghai Naiou Nano Technology Co., Ltd. The zinc powder is a granular dust and is produced by a laser method. The sample is packaged in an inert gas antistatic environment. It is sealed and stored in a dry, cool environment to prevent agglomeration caused by moisture, affecting the dispersion performance and use.

The experimental samples were scanned using a scanning electron microscope (SEM), and the results are shown in Figure 1. The sample was analyzed using a particle size analyzer. The particle size distribution of the sample is shown in Figure 2. As can be seen from Figures 1 and 2, the shape

of the zinc powder particles is mostly spherical, and although the particle size is not uniform, most of the zinc powder particles have a particle diameter of 1 μm. The zinc powder sample had the characteristics of high purity, smooth surface, large specific surface area, controllable average particle size, low bulk density, low surface oxidation, low melt deformation and low sticking into grape-like particles. The specific technical parameters are listed in Table 1.
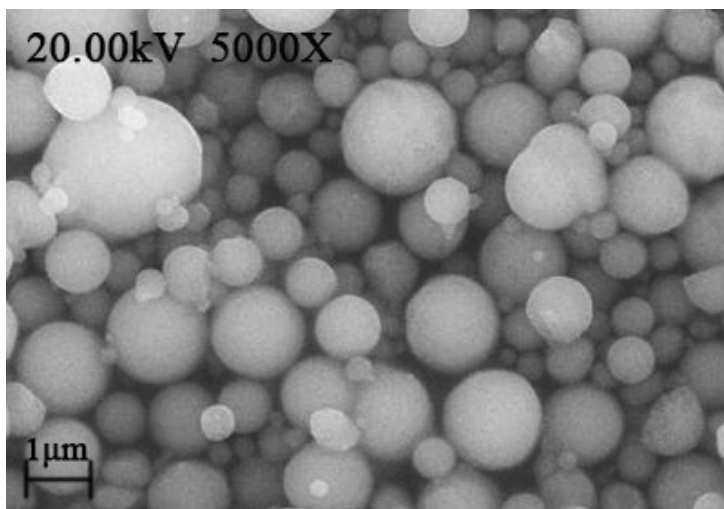


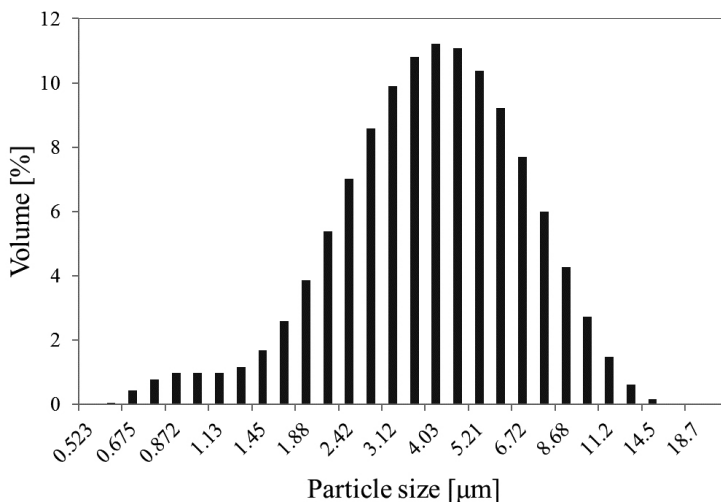**Figure 1.**    Scanning electron micrograph of zinc powder sample



**Figure 2.** Particle size distribution of zinc powder

**Table 1.** Zinc powder technical parameters (item number NO-M-003-2)

| The median particle size [μm] | Purity [%] | Specific surface area [m²/g] | Bulk density [g/cm³] | Density [g/cm³] | Crystal form | Colour |
|---|---|---|---|---|---|---|
| 3.80 | 95 | 13 | 2.0 | 7.14 | Spherical | Gray |

## 2.2. Experimental equipment

The experimental device for measurement of the gas/dust explosion parameters under special conditions (20 L sphere) was produced by Jilin Hongyuan Scientific Instrument Co., Ltd. according to the Chinese national standard [25]. It is mainly used to determine the minimum explosive concentration of a combustible gas and dust cloud in air, the maximum explosion pressure and the maximum rate of pressure increase, and the maximum explosion pressure and maximum rate of pressure increase of liquid aerosols. The device is shown in Figure 3.



**Figure 3.** 20L explosion vessel experimental device

The equipment was mainly composed of a microcomputer control system, an explosion sphere (20 L), a vacuum system, an automatic ignition device, an automatic gas distribution device, a wireless transmission system

and a computer monitoring system [26-28]. In addition, there were accessories such as wireless transmission modules, vacuum pumps, and compressed air cylinders. The specific schematic diagram is shown in Figure 4.
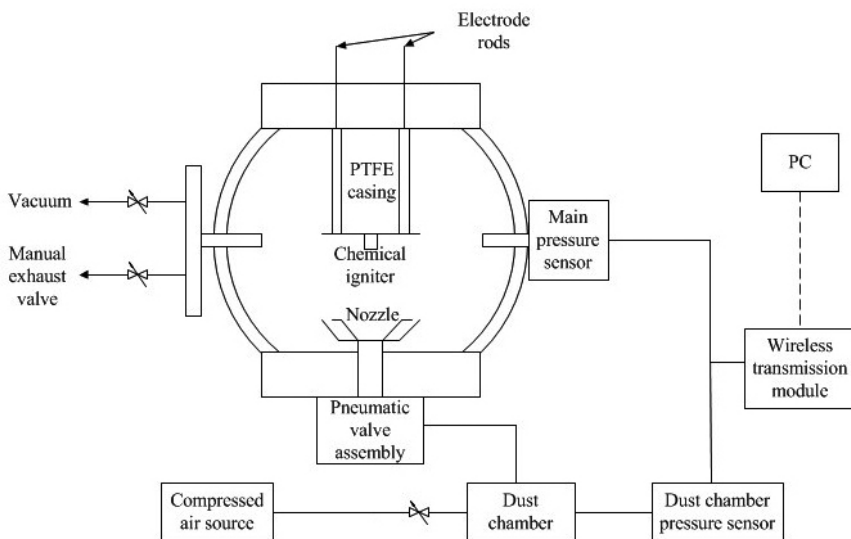


**Figure 4.**    Schematic diagram of the 20L explosion vessel experimental device

The ignition source used in this test was a chemical igniter with an ignition energy of 10 J. The chemical igniter was generally composed of zirconium powder, cerium nitrate and cerium peroxide. The mass ratio of these three materials was 4:3:3, and the explosive energy generated was 10 kJ. However, due to the high energy and high risk of the 10 kJ igniter, the electrostatic energy generated in the actual production environment was difficult to reach 10 kJ. Therefore, the maximum explosion pressure and the maximum rate of pressure increase of the tested zinc powder samples were measured with 10 J igniters. Because of the high conductivity of the metal dust, a polytetrafluoroethylene (PTFE) casing was specially customized. PTFE is a polymer obtained by polymerizing tetrafluoroethylene, and has excellent chemical stability, corrosion resistance, sealing properties, high lubricating non-stickiness and electrical insulation [29]. It was placed on the ignition electrode rod to prevent the electrode rod from breaking the uniformity of dust distribution when the electrode was energized. Its specific structure is shown in Figure 5.
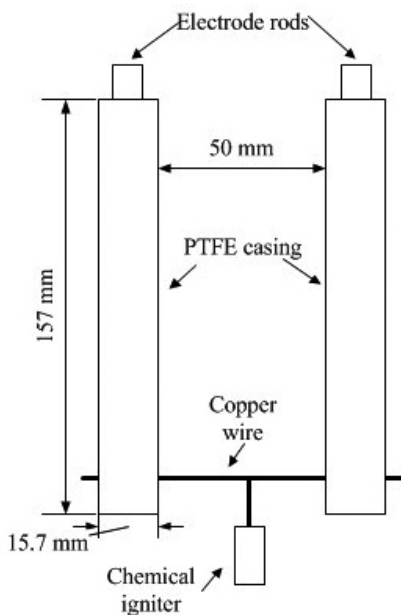
**Figure 5.**   Schematic diagram of the chemical igniter installation

## 2.3 Experimental principles

After placing a certain amount of zinc powder sample in the dust chamber of the 20 L sphere, the dust chamber is sealed. Subsequently, the 10 J chemical igniter was attached to the holder at the center of the sphere. The upper cover of the sphere is sealed and the experiment is initiated by software. The vacuum pump evacuates the sphere to the set pressure, and then the compressed air source fills the sphere with air until the pressure in the blast ball reaches 0.1 MPa. The dust chamber is pressurized to the set pressure. The dust spray solenoid valve is opened, and the igniter is ignited after the ignition delay time. Finally, the operator observes the situation inside the explosion ball through the window and collects the data produced. The pressure change during the dust explosion process is shown in Figure 6. In the figure, $t_1$ is the ignition timing of the chemical igniter, $t_2$ is the time when the dust is just ignited, $t_3$ is the time at which the maximum rate of pressure increase is generated, $t_4$ is the time at which the maximum explosion pressure is generated, and $P_0$ is the pressure generated by the chemical igniter air explosion [26, 28]. The performance of the 10 J chemical igniter used in the experiments was tested before the start of the experiments. That is, the chemical igniter is ignited without adding dust, and the explosion pressure is 0.110 MPa.
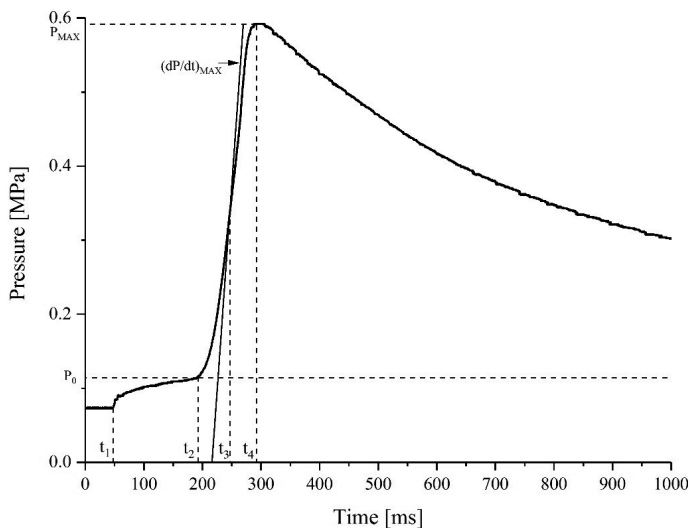
**Figure 6.**    Pressure change diagram of the dust explosion process

The operator should collect and summarize the data obtained from the dust explosion experiment. According to the data law, repeated experiments were carried out with different dust concentrations, ignition delay times and pressures for powder injection. Then the different dust concentrations, ignition delay times and maximum explosion pressures under the powder pressure were obtained. The pressure curve of the dust explosion process based on the experimental data was then constructed, and the maximum slope $(dp/dt)_{max}$ was determined. This slope is the maximum rate of pressure increase under the corresponding conditions. According to previous studies, the formula [26] for deriving the maximum rate of pressure increase $(dp/dt)_{max}$ is:

$$(\frac{dP}{dt})_{max} = 3\frac{P_{max}}{R / [S_C (P_{max} / P_0 + 1)]^{1/\gamma}} \tag{1}$$

where $S_C$ is the burning rate [m/s], $R$ is the radius of the container [m], $P_0$ is the initial pressure [Pa], and $\gamma$ is the ratio of the specific heat capacities.

## 3    Results and Discussion

### 3.1 Determination of the optimal ignition delay time

According to the sequence in the experimental method, an optimum ignition

delay time at an ambient temperature of 296.15~299.15 K, an ambient humidity of 45~55%, a pressure for powder injection of 1 MPa, and a dust concentration of 1500 g/m³ was initially obtained. The trend of the maximum explosion pressure as a function of the ignition delay time is shown in Figure 7. The trend of the maximum rate of pressure increase as a function of the ignition delay time is shown in Figure 8.

As shown in Figure 7, as the ignition delay time increases, the maximum explosion pressure of the zinc powder in the sphere changes. When the ignition delay time is 50~150 ms, the maximum explosion pressure increases with the increase in the ignition delay time. When the ignition delay time is 150~250 ms, the maximum explosion pressure ($y$) [MPa], decreases with the increase in the ignition delay time $x$ [ms]. Fitting the experimental data yields the following formula:

$$y = p_1 + p_2 lnx + p_3 (lnx)^2 + p_4 (lnx)^3 + p_5 (lnx)^4 + p_6 (lnx)^5 + p_7 (lnx)^6 + p_8 (lnx)^7 \quad (2)$$

where $p_1 = -2120.30$, $p_2 = 1224.60$, $p_3 = -23.25$, $p_4 = -86.38$, $p_5 = 1.22$, $p_6 = 6.70$, $p_7 = -1.28$, $p_8 = 0.07$. Using this formula for a two-dimensional prediction, the ignition delay time for generating the maximum explosion pressure should be 162 ms.
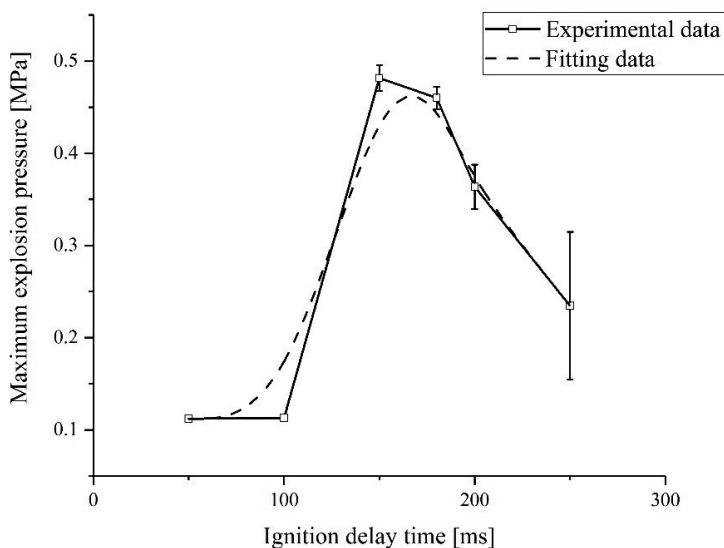


**Figure 7.**    The trend of the maximum explosion pressure *vs.* changes in the ignition delay time
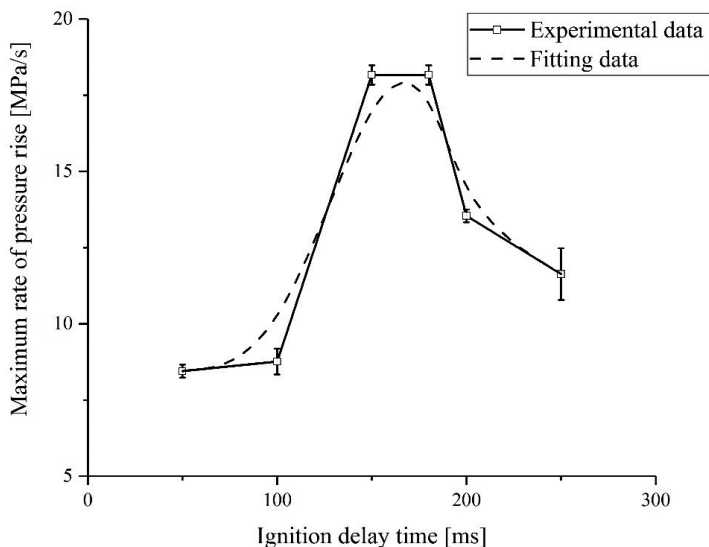
**Figure 8.** The trend of the maximum rate of pressure increase *vs.* changes in the ignition delay time

As shown in Figure 8, as the ignition delay time increases, the maximum rate of pressure increase of the zinc powder in the sphere also changes. When the ignition delay time is 50~150 ms, the maximum rate of pressure rise increases with the increase in the ignition delay time. When the ignition delay time is 150~250 ms, the maximum rate of pressure increase ($y_R$) [MPa/s] decreases with the increase in $x$. Fitting the experimental data yields the following formula:

$$y_R = p_1 + p_2 lnx + p_3(lnx)^2 + p_4(lnx)^3 + p_5(lnx)^4 + p_6(lnx)^5 + p_7(lnx)^6 + p_8(lnx)^7 \quad (3)$$

where $p_1 = -130344.47$, $p_2 = -3912.88$, $p_3 = 76661.35$, $p_4 = -35296.28$, $p_5 = 5528.94$, $p_6 = -10.40$, $p_7 = -77.22$, $p_8 = 5.49$. Using Equation 3 for a two-dimensional prediction, the ignition delay time for generating the maximum rate of pressure increase should be 165 ms. Therefore, it can be confirmed that in this case, the optimal ignition delay time of the micron-size zinc powder was 162~165 ms.

The main reason why the maximum explosion pressure and the maximum rate of pressure increase initially increases and then decreases with an increase in the ignition delay time is that the suspension state and the turbulence state of the dust change with the change in the ignition delay time. If the ignition delay time is too short, the dust will just be ejected, and will not be completely

in suspension. If the ignition delay time is too long, the dust will miss the optimal suspension state, the turbulence state will become weak, and dust deposition will begin to appear.

## 3.2 Determination of the optimal pressure for powder injection

After determining the optimal ignition delay time, the optimal pressure for powder injection was obtained at an ambient temperature of 296.15~299.15 K, an ambient humidity of 45~55%, an ignition delay time of 150 ms, and a dust concentration of 1500 g/m³. The trend of maximum explosion pressure as a function of the pressure for powder injection is shown in Figure 9. The trend of the maximum rate of pressure increase as a function of the pressure for powder injection is shown in Figure 10.
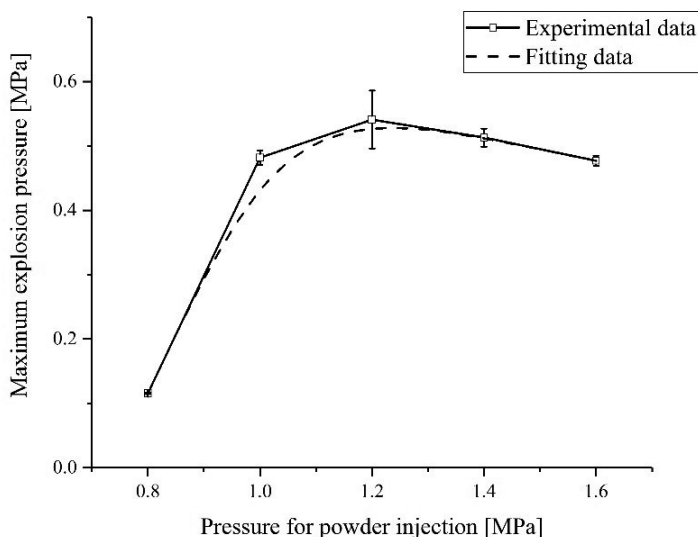


**Figure 9.**    The trend of the maximum explosion pressure *vs.* changes in the pressure for powder injection
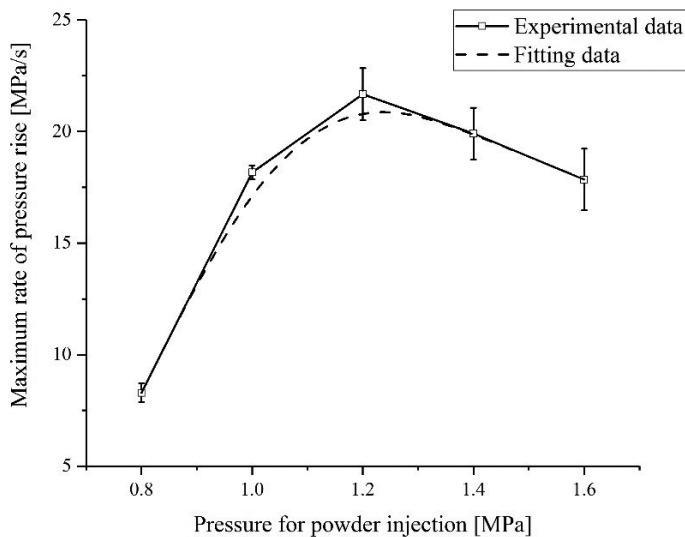
**Figure 10.** The trend of the maximum rate of pressure increase *vs.* changes in the pressure for powder injection

As shown in Figure 9, as the pressure for powder injection is continuously increased, the maximum explosion pressure of the zinc powder in the sphere changes. When the pressure for powder injection is 0.8~1.2 MPa, the maximum explosion pressure increases with the increase in the pressure for powder injection. When the pressure for powder injection ($x_I$) is 1.2~1.6 MPa, $y$ decreases with the increase in $x_I$. Fitting the experimental data yields the following formula:

$$y = p_1 e^{(-p_2 x_I)} + p_3 e^{-\left(\frac{(x_I - p_4)^2}{p_5^2}\right)} + p_6 e^{-\left(\frac{(x_I - p_7)^2}{p_8^2}\right)} \tag{4}$$

where $p_1 = 0.86$, $p_2 = 0.37$, $p_3 = -0.25$, $p_4 = 0.79$, $p_5 = -0.23$, $p_6 = -0.27$, $p_7 = 0.80$, $p_8 = -0.07$. Using Equation 4 for a two-dimensional prediction, the pressure for powder injection for generating the maximum explosion pressure should be 1.19 MPa.

As shown in Figure 10, as the pressure for powder injection is continuously increased, the maximum rate of pressure increase of the zinc powder in the sphere also changes. When the pressure for powder injection is 0.8~1.2 MPa, the maximum rate of pressure increase increases with the increase of the pressure for powder injection. When the pressure for powder injection is 1.2~1.6 MPa,

the maximum rate of pressure increase decreases with the increase in the pressure for powder injection. Fitting the experimental data yields the following formula:

$$y_R = p_1 e^{(-p_2 x_I)} + p_3 e^{-\left(\frac{(x_I - p_4)^2}{p_5^2}\right)} + p_6 e^{-\left(\frac{(x_I - p_7)^2}{p_8^2}\right)}$$  (5)

where p1 = 43.57, p2 = –0.37, p3 = 24.12, p4 = 1.06, p5 = –0.50, p6 = –78.14, p7 = 93.40, p8 = –258.34. Using Equation 5 for a two-dimensional prediction, the pressure for powder injection for generating the $y_R$ should be 1.21 MPa. Therefore, it can be confirmed that in this case, the optimal $x_I$ for the micron-sized zinc powder is 1.19~1.21 MPa.

The main reason why the maximum explosion pressure and the maximum rate of pressure increase initially increases and then decreases with the increase in the dust pressure is that the dust spray result changes with changes in the dust pressure. As the pressure for powder injection is increased, the dust in the sphere exhibits three changes in state. When the pressure for powder injection is insufficient, the dust particles cannot overcome gravity, and the sedimentation phenomenon begins to occur after the whole sphere has not been dispersed. At this time, the dust is mainly distributed in the lower half of the sphere. When the pressure for powder injection is at an optimum level, the dust is evenly distributed throughout the sphere, and the dust concentration in the entire sphere is relatively uniform. When the pressure for powder injection is too large, the dust will be driven by the powerful airflow and move rapidly in the sphere, and the dust is unevenly distributed throughout the sphere. Therefore, the maximum explosion pressure and maximum rate of pressure increase will be maximized only when the pressure for powder injection is just right.

## 3.3 Determination of the optimal dust concentration

After determining the optimal ignition delay time and the optimal pressure forpowder injection, the optimum dust concentration was obtained at an ambient temperature of 296.15~299.15 K, an ambient humidity of 45~55%, an ignition delay time of 150 ms, and a pressure for powder injection of 1.2 MPa. The trend of the maximum explosion pressure as a function of dust concentration is shown in Figure 11. The trend of the maximum rate of pressure increase as a function of dust concentration is shown in Figure 12.
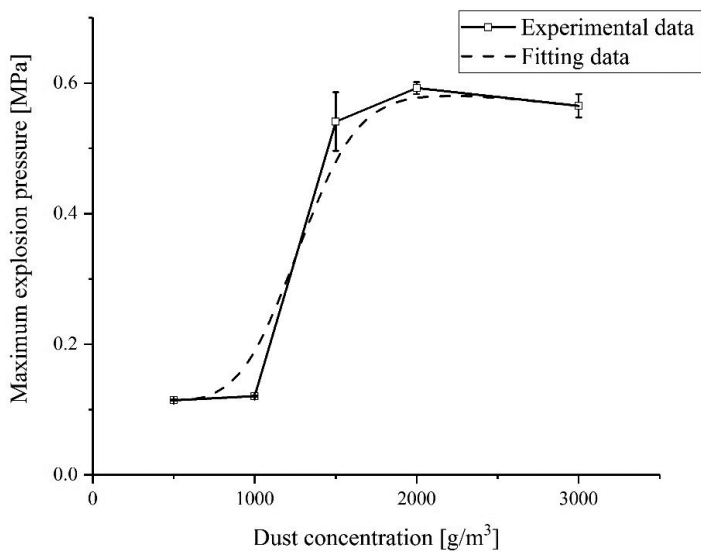
**Figure 11.** The trend of the maximum explosion pressure as a function of dust concentration
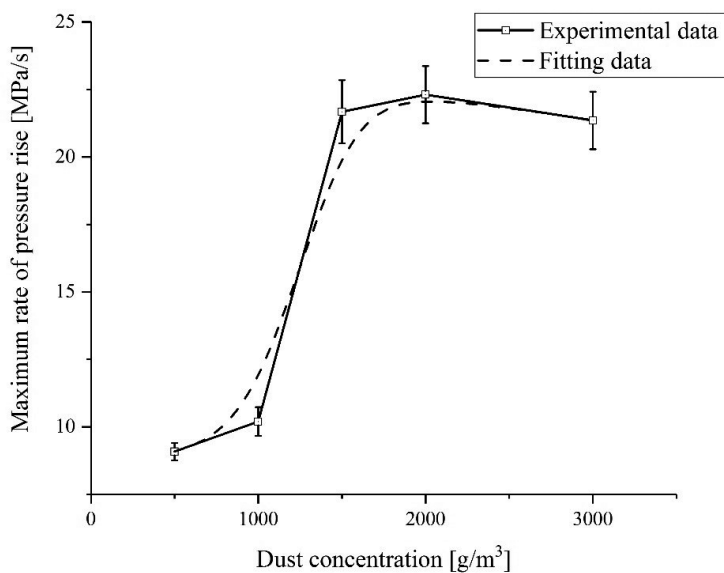


**Figure 12.** The trend of the maximum rate of pressure increase as a function of dust concentration

As shown in Figure 11, as the dust concentration is increased, the maximum explosion pressure of the zinc powder in the sphere changes. When the dust concentration is 500~2000 g/m³, the maximum explosion pressure increases with the increase in dust concentration. When the dust concentration is 2000~3000 g/m³, the maximum explosion pressure decreases with the increase in dust concentration ($d$) [g/m³]. Fitting the experimental data yields the following formula:

$$y = p_1 + p_2 d + p_3 d ln(d) + p_4 d^3 + \frac{p_5}{ln(d)} \tag{6}$$

where $p_1 = -85.36$, $p_2 = 0.12$, $p_3 = -0.014$, $p_4 = 3.17$, $p_5 = 430.81$. Using Equation 6 for a two-dimensional prediction, the dust concentration for generating the maximum explosion pressure should be 1820 g/m³.

As shown in Figure 12, as the dust concentration is increased, the maximum rate of pressure increase of the zinc powder in the sphere also changes. When the dust concentration is 500~2000 g/m³, the maximum rate of pressure increase increases with the increase in the dust concentration. When the dust concentration is 2000~3000 g/m³, the maximum rate of pressure rise decreases with the increase in dust concentration. Fitting the experimental data yields the following formula:

$$y_R = p_1 + p_2 d + p_3 d ln(d) + p_4 d^3 + \frac{p_5}{ln(d)} \tag{7}$$

where p1 = −1686.78, p2 = 0.82, p3 = −0.014, p4 = 1.34, p5 = 8915.69. Using Equation 7 for a two-dimensional prediction, the dust concentration for generating the maximum rate of pressure increase should be 1750 g/m³. Therefore, it can be confirmed that in this case, the optimal dust concentration of the micron-sized zinc powder is 1750~1820 g/m³.

The main reason why the maximum explosion pressure and the maximum rate of pressure increase initially increases and then decreases with the increase in dust concentration is that when the dust concentration in the sphere is low, the oxygen in the sphere is sufficient, so that all the dust can be burned and exploded. Therefore, by increasing the dust concentration, the amount of dust particles participating in the reaction increases, the heat released by the reaction increases, and the heat released per unit time also increases. This means that the maximum explosion pressure and the maximum rate of pressure increase of the dust becomes larger. When the dust concentration exceeds a certain value, the oxygen in the sphere is insufficient. The number of dust particles participating

in the reaction per unit volume is reduced, the heat released by the reaction is reduced, and the heat released per unit time is also reduced. This means that the maximum explosion pressure and maximum rate of pressure increase of the dust are reduced. In addition, when the dust concentration is too large, the number of particles that do not participate in the combustion reaction around the combustion particles increases relatively. They absorb the heat generated by the explosion, causing the sensor's perceived heat to drop overall. This results in a decrease in the maximum explosion pressure and maximum rate of pressure increase.

## 3.4 The order of influence of three factors on the explosion intensity parameters of micron-sized zinc powder

In order to study the influence of three factors (dust concentration, ignition delay time, pressure for powder injection) on the explosion intensity parameters of micron-sized zinc powder (maximum explosion pressure and maximum rate of pressure increase), the experimental data were grouped according to changes of two of the three factors, that is, one factor in each group is unchanged, and the other two factors are changed. Finally the data were divided into 6 groups. They were:

*i*)    the influence of dust concentration and the pressure for powder injection on the maximum explosion pressure,

*ii*)   the influence of dust concentration and ignition delay time on the maximum explosion pressure,

*iii*)  the influence of ignition delay time and the pressure for powder injection on the maximum explosion pressure,

*iv*)  the influence of dust concentration and the pressure for powder injection on the maximum rate of pressure increase,

*v*)   the influence of dust concentration and ignition delay time on the maximum rate of pressure increase,

*vi*)  the influence of ignition delay time and the pressure for powder injection on the maximum rate of pressure increase.

    The 6 groups of data were then fitted respectively. The following six figures were obtained.
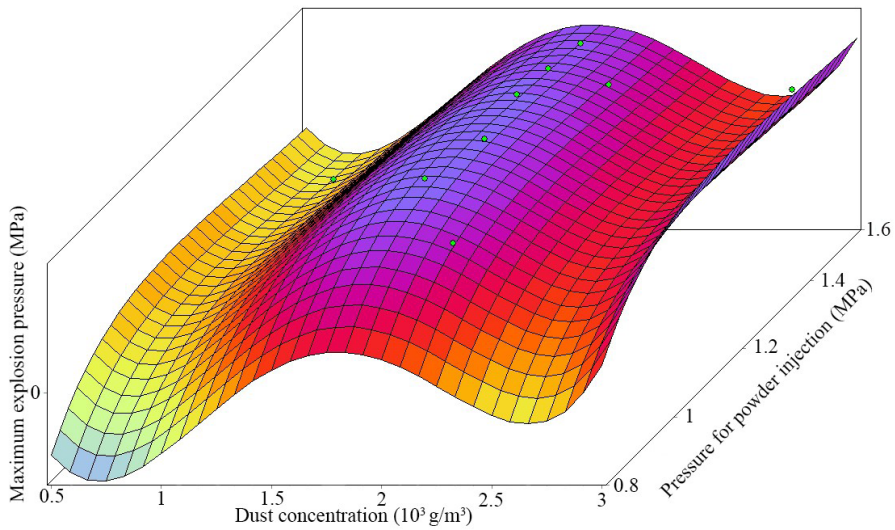
**Figure 13.** The influence of dust concentration and the pressure for powder injection on the maximum explosion pressure
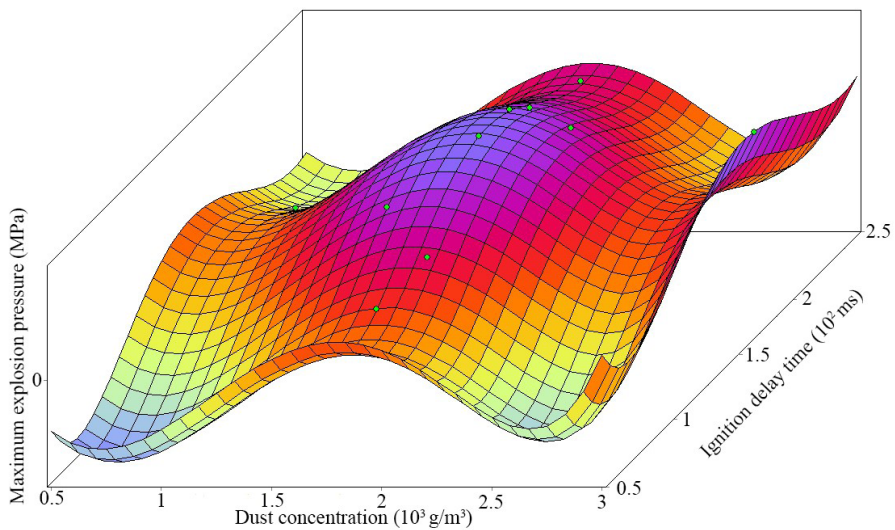


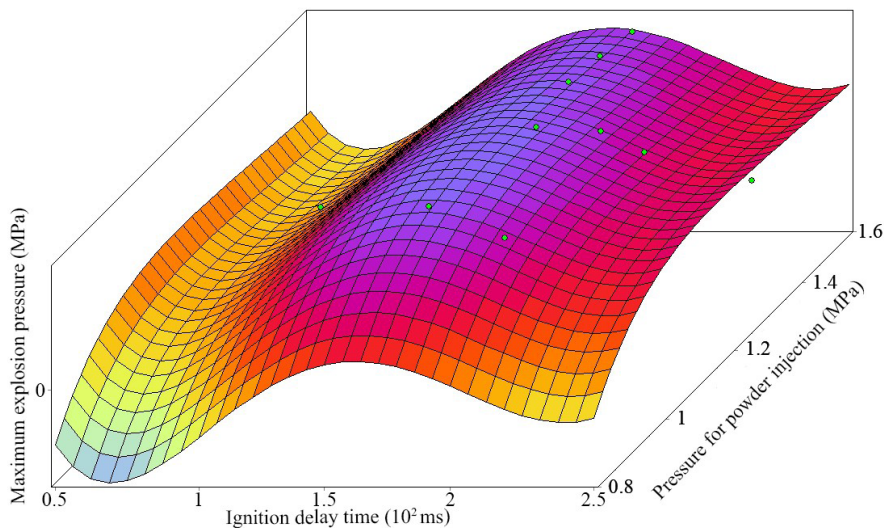**Figure 14.** The influence of dust concentration and ignition delay time on the maximum explosion pressure

**Figure 15.** The influence of ignition delay time and the pressure for powder injection on the maximum explosion pressure
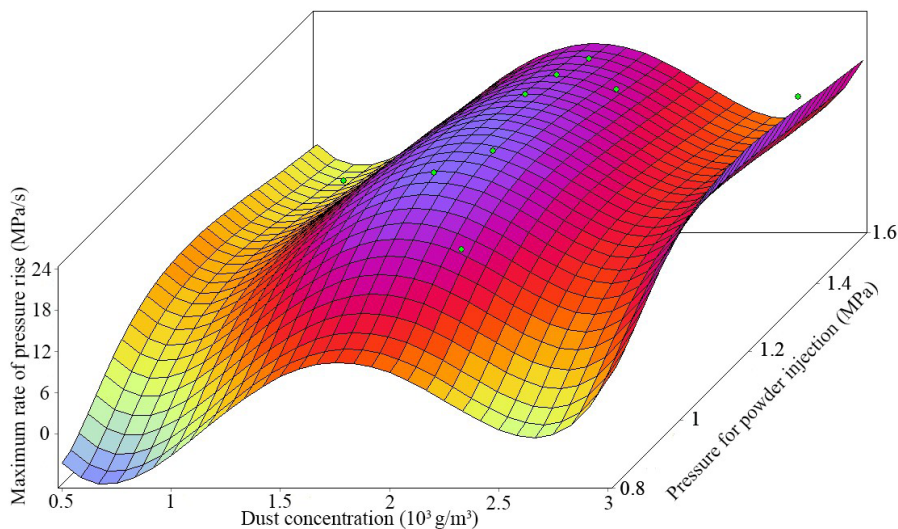


**Figure 16.** The influence of dust concentration and the pressure for powder injection on the maximum rate of pressure increase
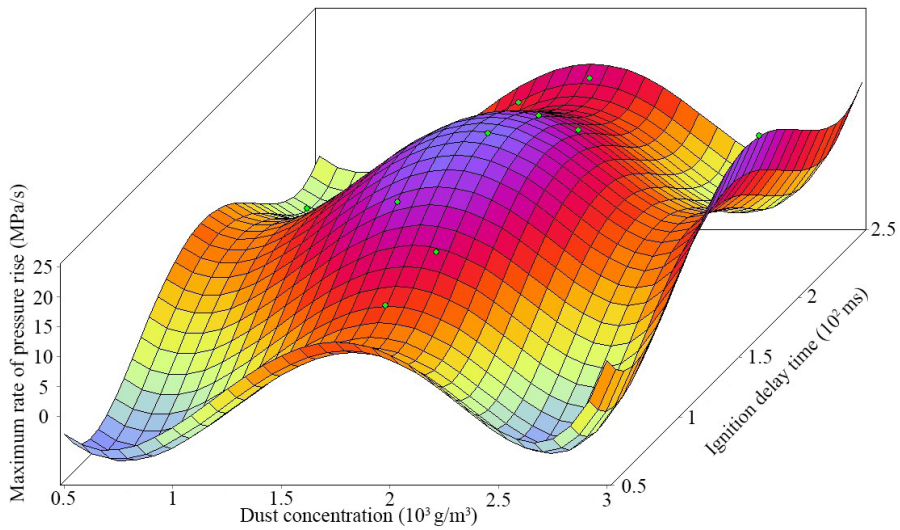
**Figure 17.** The influence of dust concentration and ignition delay time on the maximum rate of pressure increase
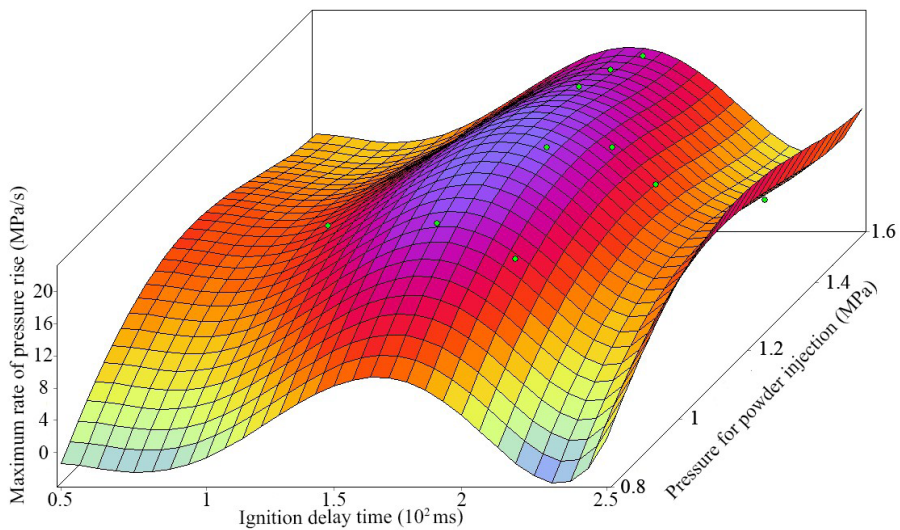


**Figure 18.** The influence of ignition delay time and the pressure for powder injection on the maximum rate of pressure increase

As can be seen from Figure 13, when the $d$ value is constant, the change in the $x_I$ value contributes less to the change in the $y$ value. When the $x_I$ value is constant, the change of $d$ value contributes a lot to the change of $y$ value. Therefore, it can be deduced that the influence of the dust concentration on the maximum explosion pressure is greater than the influence of the pressure for powder injection on the maximum explosion pressure. Similarly, according to Figure 14, it can be deduced that the influence of the dust concentration on the maximum explosion pressure is greater than the influence of the ignition delay time on the maximum explosion pressure. According to Figure 15, it can be deduced that the influence of the ignition delay time on the maximum explosion pressure is greater than the influence of the pressure for powder injection on the maximum explosion pressure. In summary, the degree of influence of the three factors on the maximum explosion pressure is: dust concentration > ignition delay time > pressure for powder injection.

According to the above analysis method, analysis of Figures 16 to 18 yielded similar conclusions. The degree of influence of the three factors on the maximum rate of pressure increase is: dust concentration, ignition delay time, pressure for powder injection.

## 3.5  Discussion

The purpose of these experiments was to study the explosion hazard of micron-sized zinc powder existing in the small space and low energy environments such as the actual ventilation pipes of zinc powder processing plants. Therefore, micron-sized zinc powder was subjected to dust explosion experiments using a small energy chemical igniter. Although the experimental data is more suitable for micron-sized zinc powder explosion scenes, that may occur in actual production, the ignition energy is low, which may lead to incomplete combustion of the experimental dust, resulting in low experimental pressure data.

In order to solve the possible situation of the burning of experimental dust samples, component analysis of the post-explosion residues will be added in future experiments. By analyzing the composition of the residue after an explosion, the proportion of zinc powder involved in the experiment and the concentration of dust that ensures complete combustion of the sample can be obtained. Through the statistics and analysis of the data, a modified parameter formula for the experimental pressure data is obtained, which makes the dust explosion intensity data of the micron-sized zinc powder more valuable.

# 4 Conclusions

The purpose of this study was to study the explosion hazard of micron-sized zinc powder in a small space and low energy environment in actual ventilation pipes in zinc powder processing plants. Through experiment and data analysis, the explosion violence intensity parameters of micron-sized zinc powder dust were obtained. The results obtained were as follows:

a) The experimental conditions were an ambient temperature of 296.15~299.15 K, an ambient humidity of 45~55%, and an ignition energy of 10 J. When the ignition delay time was 150 ms, the pressure for powder injection was 1.2 MPa, and the dust concentration was 2000 g/m$^3$, the explosion pressure and rate of pressure increase of the micron-sized zinc powder dust explosion reached their maximum values. This maximum explosion pressure was 0.482 ±0.013 MPa. The maximum rate of pressure increase was 22.310 ±1.594 MPa/s.

b) When the ignition energy is 10 J and the explosion violence parameters of micron-sized zinc powder dust is the highest, the ignition delay time should be 162~165 ms, the pressure for powder injection should be 1.19~1.21 MPa, and the dust concentration 1750~1820 g/m$^3$.

c) The experimental data were grouped according to changes in two of three factors, and they were divided into 6 groups. The data of each group were then processed by the fitting method, and the degree of influence of the three factors on the explosion intensity parameters of micron-sized zinc powder (maximum explosion pressure and maximum rate of pressure increase) were ranked as follows:
dust concentration > ignition delay time > pressure for powder injection.

d) The results of the experimental data are more suitable for small space, micron-sized and the low energy environment existing in the ventilation pipes of zinc powder processing plants. However, due to the low ignition energy, the experimental dust may not be completely burned, resulting in low experimental pressure data.

# References

[1]  Song, Y.; Nassim, B.; Zhang, Q. Explosion Energy of Methane/Deposited Coal Dust and Inert Effects of Rock Dust. *Fuel* **2018**, *228*: 112-122.

[2]  Fu, B.; Liu, G.; Sun, M.; Hower, J.C.; Hu, G.; Wu, D. A Comparative Study on the Mineralogy, Chemical Speciation, and Combustion Behavior of Toxic Elements of Coal Beneficiation Products. *Fuel* **2018**, *228*: 297-308.

[3]  Ni, P.; Bai, L.; Wang, X.; Li, R. Characteristics of Evolution of In-Cylinder Soot Particle Size and Number Density in a Diesel Engine. *Fuel* **2018**, *228*: 215-225.

[4]  Lanzerstorfer, C. Fly Ash From Coal Combustion: Dependence of the Concentration of Various Elements on the Particle Size. *Fuel* **2018**, *228*: 263-271.

[5]  Fedorov, A.V.; Shulgin, A.V. About Stability of the Ignition Process of Small Solid Particle. *J. Loss Prev. Process Ind.* **2007**, *20*(4-6): 317-321.

[6]  Xiao, H.; Sun, J.; He, X. A Study on the Dynamic Behavior of Premixed Propane-Air Flames Propagating in a Curved Combustion Chamber. *Fuel* **2018**, *228*: 342-348.

[7]  Klinzing, G.E.; Basha, O.M. A Correlation for Particle Velocities in Pneumatic Conveying. *Powder Technol.* **2017**, *310*: 201-204.

[8]  Cashdollar, K.L. Coal Dust Explosibility. *J. Loss Prev. Process Ind.* **1996**, *9*(1): 65-76.

[9]  Cao, W.; Gao, W.; Peng, Y.; Liang, J.; Pan, F.; Xu, S. Experimental and Numerical Study on Flame Propagation Behaviors in Coal Dust Explosions. *Powder Technol.* **2014**, *266*: 456-462.

[10] Cashdollar, K.L. Overview of Dust Explosibility Characteristics. *J. Loss Prev. Process Ind.* **2000**, *13*: 183-199.

[11] Joseph, G.; Team, C.S.B.H.I. Combustible Dusts: a Serious Industrial Hazard. *J. Hazard. Mater.* **2007**, *142*(3): 589-91.

[12] Cao, W.; Gao, W.; Liang, J.; Xu, S.; Pan, F. Flame-Propagation Behavior and a Dynamic Model for the Thermal-radiation Effects in Coal-Dust Explosions. *J. Loss Prev. Process Ind.* **2014**, *29*: 65-71.

[13] Di Sarli, V.; Russo, P.; Sanchirico, R.; Di Benedetto, A. CFD Simulations of Dust Dispersion in the 20 L Vessel: Effect of Nominal Dust Concentration. *J. Loss Prev. Process Ind.* **2014**, *27*: 8-12.

[14] Mishra, K.B.; Wehrstedt, K.-D. Spill-Over Characteristics of Peroxy-Fuels: Two-Phase CFD Investigations. *J. Loss Prev. Process Ind.* **2014**, *29*: 186-197.

[15] Shen, Y.S.; Yu, A.B.; Austin, P.R.; Zulli, P. CFD Study of In-Furnace Phenomena of Pulverised Coal Injection in Blast Furnace: Effects of Operating Conditions. *Powder Technol.* **2012**, *223*: 27-38.

[16] Yan, X.; Yu, J. Dust Explosion Venting of Small Vessels at the Elevated Static Activation Overpressure. *Powder Technol.* **2014**, *261*: 250-256.

[17] Xiao, H.; Sun, J.; Chen, P. Experimental and Numerical Study of Premixed Hydrogen/Air Flame Propagating in a Combustion Chamber. *J. Hazard. Mater.* **2014**, *268*: 132-9.

[18] Xin, H.-h.; Wang, D.-m.; Qi, X.-y.; Qi, G.-s.; Dou, G.-l. Structural Characteristics

of Coal Functional Groups Using Quantum Chemistry for Quantification of Infrared Spectra. *Fuel Process Technol.* **2014**, *118*: 287-295.

[19] Li, Q.; Wang, K.; Zheng, Y.; Mei, X.; Lin, B. Explosion Severity of Micro-Sized Aluminum Dust and Its Flame Propagation Properties in 20 L Spherical Vessel. *Powder Technol.* **2016**, *301*: 1299-1308.

[20] Zhang, Q.; Liu, L.; Shen, S. Effect of Turbulence on Explosion of Aluminum Dust at Various Concentrations in Air. *Powder Technol.* **2018**, *325*: 467-475.

[21] Choi, K.; Sakasai, H.; Nishimura, K. Minimum Ignition Energies of Pure Magnesium Powders Due to Electrostatic Discharges and Nitrogen's Effect. *J. Loss Prev. Process Ind.* **2016**, *41*: 144-146.

[22] Marmo, L.; Piccinini, N.; Danzi, E. Small Magnitude Explosion of Aluminium Powder in an Abatement Plant: A Telling Case. *Process Saf. Environ. Prot.* **2015**, *98*: 221-230.

[23] Li, Q.; Lin, B.; Dai, H.; Zhao, S. Explosion Characteristics of $H_2$/$CH_4$/Air and $CH_4$/Coal Dust/Air Mixtures. *Powder Technol.* **2012**, *229*: 222-228.

[24] Cao, W.; Cao, W.; Peng, Y.; Qiu, S.; Miao, N.; Pan, F. Experimental Study on the Combustion Sensitivity Parameters and Pre-combusted Changes in Functional Groups of Lignite Coal Dust. *Powder Technol.* **2015**, *283*: 512-518.

[25] GB/T 16426-1996 *Determination for Maximum Explosion Pressure and Maximum Rate of Pressure Rise of Dust Cloud.* (in Chinese).

[26] Proust, C.; Accorsi, A.; Dupont, L. Measuring the Violence of Dust Explosions with the "20l Sphere" and with the Standard "ISO 1 m³ Vessel". *J. Loss Prev. Process Ind.* **2007**, *20*(4-6): 599-606.

[27] Dahoe, A.E.; Cant, R.S.; Pegg, M.J.; Scarlett, B. On the Transient Flow in the 20-Liter Explosion Sphere. *J. Loss Prev. Process Ind.* **2001**, *14*: 475-487.

[28] Cao, W.; Qin, Q.; Cao, W.; Lan, Y.; Chen, T.; Xu, S.; Cao, X. Experimental and Numerical Studies on the Explosion Severities of Coal Dust/Air Mixtures in a 20-L Spherical Vessel. *Powder Technol.* **2017**, *310*: 17-23.

[29] Mnif, R.; Ben Jemaa, M.C.; Kacem, N.H.; Elleuch, R. Impact of Viscoelasticity on the Tribological Behavior of PTFE Composites for Valve Seals Application. *Tribology Trans.* **2013**, *56*(5): 879-886.